Low repetition rate 343 nm passively Q-switched solid-state laser for time-resolved fluorescence spectroscopy

Rodenko, Olga; Tidemand-Lichtenberg, Peter; Pedersen, Christian

Published in:
Optics Express

Link to article, DOI:
10.1364/OE.26.020614

Publication date:
2018

Document Version
Publisher's PDF, also known as Version of record

Research Article | Vol. 26, No. 16 | 6 Aug 2018 | OPTICS EXPRESS 20614
Optics EXPRESS

Low repetition rate 343 nm passively Q-switched solid-state laser for time-resolved fluorescence spectroscopy

OLGA RODENKO,[1,2,*] PETER TIDEMAND-LICHTENBERG,[1] AND CHRISTIAN PEDERSEN[1]

[1]*Technical University of Denmark, Frederiksborgvej 399, 4000 Roskilde, Denmark*
[2]*Radiometer Medical ApS, Åkandevej 21, 2700 Brønshøj, Denmark*
[*]*olro@fotonik.dtu.dk*

Abstract: We demonstrate a low-cost 343 nm solid-state laser delivering up to 20 µJ per pulse, with a pulse width of 2.3 ns at a repetition rate of 100 Hz. The 343 nm is obtained through a third harmonic generation of a passively Q-switched 1030 nm Yb:YAG laser with pulse energy of 190 µJ at 100 Hz and a pulse width of 5.4 ns. The IR-UV conversion efficiency is 10.4%, comparable to that achieved with mode-locked IR lasers. The light source is electronically controlled for easy synchronization with a detection circuit. The low repetition rate specifically targets applications exploiting the millisecond scale lifetime of lanthanides employed in fluoroimmunoassay measurements for time-resolved fluorescence spectroscopy. Low repetition rate and even pulse-on-demand operation is demonstrated.

1. Introduction

An excitation wavelength of 343 nm matches the absorption peaks of many fluorophores, including long lifetime lanthanides (europium, terbium) [1] and other nanosecond scale lifetime biological markers such as NADH [2]. This circumstance motivates us to develop a laser at 343 nm for fluorescence spectroscopy applications.

Lanthanides have been mostly excited by flash lamps [1]. The Xenon flash lamp such as the 5 W L9455 by Hamamatsu, employed in a state-of-the-art flash lamp based time-resolved system, emits 5 µJ per pulse in the spectral range of 300-394 nm [3]. In this work we aim to obtain at least the same pulse energy with a solid-state UV laser. The narrow (<1 nm) spectral bandwidth of the laser allows precise targeting of the lanthanides absorption peak. Moreover, the spatial beam quality of the laser enables easy light shaping and additionally makes 2D scanning of a sample possible with high spatial resolution. We believe the precise spectral and spatial targeting of lanthanide fluorophores will allow for improved signal-to-noise-ratios in fluoroimmunoassay measurements.

One approach to obtain a UV light source is to use a cascade of nonlinear conversion processes from the infrared to the UV wavelength to generate the third harmonic of a solid-state laser. Laser transitions of an Yb:YAG crystal allow for emission at the 1030 nm wavelength, which can then be tripled to obtain the desired 343 nm. The long upper state lifetime of Yb:YAG (1 ms) promotes high pulse energies and low repetition rates in a Q-switched configuration. Other advantages of Yb:YAG crystals are the small quantum defect and relatively simple energy level diagram, however, the latter at the same time leads to reabsorption due to quasi-three-level operation. Advantages of passively Q-switched lasers include simplicity, cost-effectiveness and compactness compared to actively pulsed light sources. Here we demonstrate, that through the control of the repetition rate of a pulsed pumped passively Q-switched laser, the generated pulses can be conveniently synchronized with a detection system in time-resolved fluorescence measurements, without complex electronics. The low repetition rate is required to avoid cross talk between successive measurements when using lanthanides with long fluorescence lifetime (approximately 1 ms).

#334724 https://doi.org/10.1364/OE.26.020614
Journal © 2018 Received 8 Jun 2018; revised 15 Jul 2018; accepted 17 Jul 2018; published 27 Jul 2018

Optics EXPRESS

Such low repetition rates cannot be obtained with mode locked lasers without using pulse pickers [4].

At 343 nm, the following pulse energies have been obtained: 28.6 µJ at a repetition rate of 3.5 MHz, obtained from a mode locked IR laser delivering 177 µJ and a peak power of 240 MW, corresponding to IR-UV conversion efficiency of 16% [5], 780 µJ at 300 kHz, pumped with a mode locked thin disk laser amplifier with 4.7 mJ and a peak power of 590 MW, corresponding to IR-UV conversion efficiency of 17% [6]. These laser sources possess high degree of complexity and are therefore expensive. In addition, the high peak power of mode locked lasers promotes high conversion efficiency of the third harmonic generation.

High-power passively Q-switched Yb:YAG/Cr^{4+}:YAG lasers have been demonstrated [7]. The highest pulse energies at 1030 nm have been achieved with composite Yb:YAG/Cr^{4+}:YAG microchip lasers: 1.6 mJ at a repetition rate of 50 Hz (pumped with 86 mJ at 50 Hz and a peak diode power of 100 W) [8], 3.6 mJ (pumped with 60 mJ at 20 Hz and peak diode power of 120 W) [9]. Third harmonic generation of passive Q-switched 1064 nm lasers has been demonstrated generating 355 nm with pulse energies of 57 µJ at 38.6 kHz [10]. To the authors' best knowledge, the generation of 343 nm in passive Q-switched lasers has not been reported. This work presents a low-cost and simple 343 nm solid-state laser system with controllable repetition rate and pulse energies sufficient for a range of fluorescence spectroscopy applications.

We demonstrate a pulse energy of 20 µJ (2.3 ns pulse width) at 343 nm when operating at the target repetition rate of 100 Hz, converted from a 1030 nm laser pulse of 190 µJ and peak power of 33 kW. The IR to UV conversion efficiency is 10.4% which is comparable to that obtained with mode locked lasers. The controllable repetition rate allows the emission of pulses on demand and easy synchronization with a detection circuit. The low repetition rate matches the requirements for use with long lifetime lanthanide fluorophores, whereas the laser output spectrum matches their excitation peak. The laser is simple and provides a low-cost solution compared to other solid-state laser solutions. We also show that the impact of timing jitter from this laser is negligible for lanthanide time-resolved fluorescence spectroscopy. For fast fluorophores with decay time at nanosecond scale, an optical feedback synchronization circuit will allow for the use of the presented laser source.

2. Experimental setup

The experimental setup is shown in Fig. 1. The pump diode (LD) is manufactured by Lumentum Operations LLC with a center wavelength of 940 nm. The fiber core diameter is 105 µm, with a 0.15 NA and power output of up to 10.6 W. The laser diode is externally triggered at a repetition rate of 10 to 180 Hz and with a fixed pulse width of 2 ms. The pump pulse width is limited by the output power of the laser diode. The pulse width of 2 ms is chosen to reach the pump energy threshold while operating at the maximum specified current of 12 A. The same electronic trigger signal can also be used for a detection circuit relevant for our target application. The diode pump energy is 21 mJ per pulse with a peak power of 10.6 W. At 100 Hz, the average power is then 2.12 W. The laser diode is operated at a constant temperature of 18°C. The light emitted from the pump diode is focused into the laser crystal with a magnification of 3.33 (lens system L1) resulting in a pump beam diameter of 350 µm. The laser crystal (10%Yb:YAG) is manufactured by Castech Inc. and has a transverse dimension of 5x5 mm^2 and a thickness of 3 mm. The laser crystal is wrapped in indium foil to improve thermal conductivity at the interface between the crystal and the heat sink. The laser crystal is coated: HR@1030 nm and HT@940 nm at the front surface facing the pump diode and AR@1030 nm at the intracavity surface. A temperature controller keeps the temperature of the laser crystal fixed at 15°C. For a quasi-three-level gain medium keeping the temperature low is highly important as the population of the lower laser level increases with temperature thus reducing the laser efficiency. A Cr^{4+}:YAG crystal is employed as a saturable absorber enforcing Q-switched operation of the laser. The Cr^{4+}:YAG crystal is manufactured

Optics EXPRESS

by FEE GmbH and measures 5x5x1 mm^3 designed for a small signal transmission of 90% when installed at Brewster's angle. The saturable absorber is placed approximately 6 mm after the laser crystal at Brewster's angle to enforce a linearly polarized output. The output coupler (OC) is a plane mirror with 60% reflection at 1030 nm. The cavity length is in total 13 mm (optical length).

Second harmonic (SHG) and sum frequency generation (SFG) is obtained with LBO crystals. LBO is selected due to its high optical damage threshold and relatively large angular acceptance bandwidths [11]. The second harmonic to 515 nm is obtained with a 15 mm long LBO crystal kept at 193°C (LBO1) using noncritical phase matching (NCPM). The 1030 nm laser beam is focused into the LBO1 crystal with a magnification of 1.25 (lens system L2) relative to the beam size in the laser cavity. For the SFG stage both the 1030 nm and 515 nm laser beams, respectively, are focused with a magnification of unity in the center of a 20 mm long LBO crystal kept at 18°C (LBO2), with a cut angle of 50.1°. The SFG crystal is cut for type II critical phase matching.

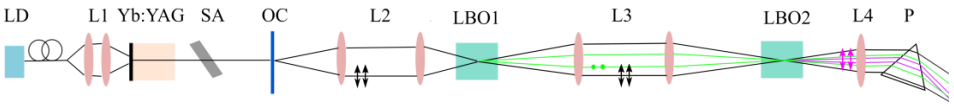

Fig. 1. Experimental setup including the diode laser (LD), the Yb:YAG laser crystal, the Cr^{4+}:YAG saturable absorber (SA), the laser output mirror (OC), lens systems (L1-L4), two LBO crystals and a dispersive prism (P).

3. Results and discussion

3.1. Passively Q-switched 1030 nm laser

An important feature is that the repetition rate of the Q-switched laser is controllable and dictated by the trigger circuit for the pump diode. We have therefore characterized the Yb:YAG laser operation as a function of repetition rate.

The generated spectra are measured with an optical spectrum analyzer (OSA) AQ6317B with a resolution of 50 pm. The pulse duration (FWHM) is measured with a Melles Griot detector 13DAH001 with a bandwidth of 3 GHz and an oscilloscope WaveSurfer 104Xs with a bandwidth of 1 GHz. The optical spectrum of the passively Q-switched laser is centered at 1029.94 nm with a full width at half maximum (FWHM) of 0.33 nm measured at a repetition rate of 100 Hz, as shown in Fig. 2(a). The linewidth is measured with no additional frequency selective element inserted in the cavity. Varying the repetition rate from 10 Hz to 180 Hz, the center wavelength is found to fluctuate in the range 1029.94-1030.68 nm, shown in inset figure in Fig. 2(a), while the emission bandwidth remains constant. The spectral width would be reduced and stabilized using a frequency selective element locking the output spectrum and center wavelength. The calculated SHG conversion efficiency as a function of wavelength is also shown in Fig. 2. For the calculation we used a 15 mm long NCPM LBO crystal at 193°C and a beam radius of 156 μm. The model is described later in text. The calculated spectral acceptance bandwidth FWHM is 1.8 nm which is about five times wider than the bandwidth of the laser emission. The optical spectrum of the 515 nm output is centered at 515.28 nm with a FWHM of 0.27 nm, see Fig. 2(b). The optical spectrum of the 343 nm output is not measured since it was beyond the spectral range of the OSA available. However, the spectrum of the 343 nm beam is the convolution of the interacting beams, 1030 nm and 515 nm. Thus, the FWHM of the UV spectrum is below 0.2 nm.

Optics EXPRESS

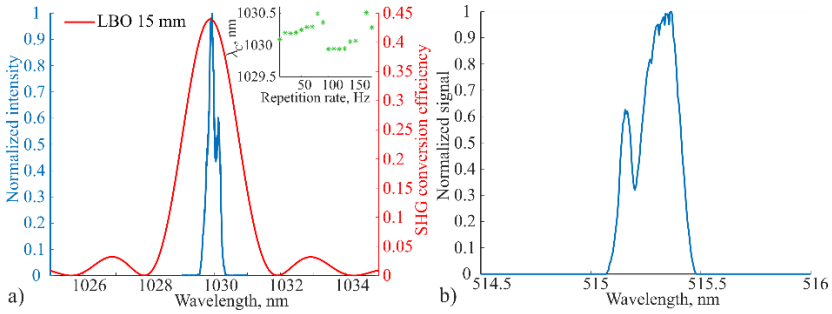

Fig. 2. a) Spectrum of the 1030 nm output centered at 1029.94 nm with a FWHM of 0.33 nm measured at 100 Hz, and calculated conversion efficiency as a function of wavelength with the spectral acceptance bandwidth of 1.8 nm; inset: center wavelength as a function of repetition rate; b) spectrum of the 515 nm output centered at 515.28 nm with a FWHM of 0.27 nm.

The pulse energy at 1030 nm monotonously increases from 142 µJ at 10 Hz to 204 µJ at 180 Hz, as shown in Fig. 3(a). The pulse energy is calculated from measured average power and repetition rate. We believe the reason of the pulse energy growing with the repetition rate is the following. With increasing repetition rate, the thermal load increases and the crystal temperature rises because of higher incident pump energy. The stimulated emission cross-section of the laser medium decreases with temperature [12], which was experimentally confirmed in [12,13]. According to these references, higher population inversion is needed to reach the threshold, hence a pulse with higher energy is emitted. This explanation was also confirmed by measurement of the delay time of the Q-switched pulse relative to the leading edge of the pump diode pulse: the delay time increases with higher repetition rate, thus with the higher thermal load, so that the Q-switched pulse is emitted later, which can be seen in the inset in Fig. 3(a). With the increased delay time, more pump energy is stored in the gain medium before the emission of the pulse, corresponding to larger pump energy threshold, resulting in larger pulse energy of the Q-switched pulse. Interestingly, starting approximately at the repetition rate of 130 Hz the Q-switched pulse is emitted after the end of the pump diode pulse. Another effect which could reduce the pulse energy, is the temperature dependence of the SA transmission. However, it has been demonstrated that this effect is negligible [14].

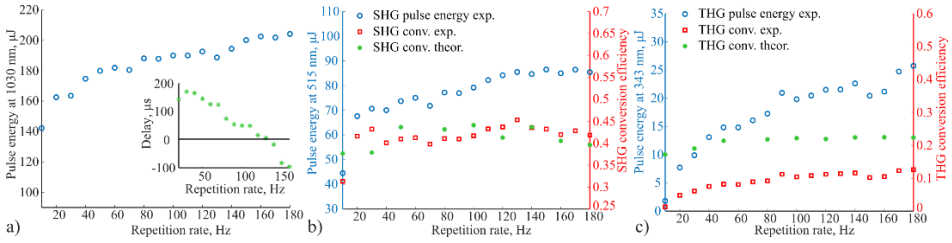

Fig. 3. a) Pulse energy of the 1030 nm output as a function of repetition rate; inset: delay of the emitted Q-switched pulse relative to the falling edge of the pump pulse; b) pulse energy at the 515 nm output (blue), and SHG conversion efficiency as a function of repetition rate, measured (red) and calculated (green); c) pulse energy of the 343 nm output (blue), and IR-UV conversion efficiency, measured (red) and calculated (green).

The upper lasing limit of our system is 250 Hz, which corresponds to the average incident pump power of 5 W and the pump diode duty cycle of 50%. Operation at higher repetition frequencies is hampered by the thermal load on the laser crystal. Therefore, the Q-switched laser operation with a continuous pumping cannot be obtained because of too high thermal load. At the same time, there is no lower limit of the laser repetition rate. The system can emit single Q-switched pulses on demand using single pump pulses. Potentially, the repetition rate operation range can be extended by improving the thermal design of the system. The peak

Optics EXPRESS

power at 1030 nm is in the range of 25 to 36 kW at 10 to 180 Hz assuming a Gaussian pulse shape. The pulse width fluctuates only about 6.8% when changing the repetition rate, however, without clear correlation to the repetition rate, see inset in Fig. 4(a). Although the infrared laser operates up to 250 Hz, the harmonic generation is measured only up to 180 Hz, as higher repetition rates lead to damage of the achromatic lenses L3.

The beam waist is measured as a function of repetition rate in Q-switched operation with the knife-edge method (data not shown). The measured beam waist (radius) does not change significantly with the repetition rate and is in the range from 121 µm at 10 Hz to 139 µm at 180 Hz. The measured beam radius is 123.7 µm at 100 Hz.

3.2. Third harmonic generation

A numerical model is used to predict the SHG and THG conversion efficiencies. The model is based on the coupled wave theory [15]. Using the plane wave approximation (large beam size), and considering quasi-stationary fields (long temporal pulses) it is possible to calculate SHG and SFG power conversion efficiencies as shown in Fig. 3(b) and 3(c), respectively, by integration of temporal pulses. Furthermore, the beam walk-off is included in the SFG calculations. The measured values of beam size, peak power and pulse duration of the fundamental 1030 nm beam are used as input parameters in the model. The refractive indices are calculated as in [16] with the temperature dependence from [17]. The effective nonlinear coefficients are taken from [18].

The pulse energy of the 515 nm output increases from 45 µJ at 10 Hz to 87 µJ at 180 Hz. The measured SHG conversion efficiency exhibits rather constant behavior in the range of 40-45%, see Fig. 3(b), red squares. It should be noted, that the SHG crystal was slightly angle readjusted to compensate for the fluctuating center wavelength of the infrared laser and varying temperatures for different repetition rates, as shown earlier in the paper, see inset in Fig. 2(a). The SHG conversion efficiency is calculated to be 44% at 100 Hz and does not change with the repetition rate, see Fig. 3(b), green dots, calculated based on measured beam sizes and peak powers as a function of repetition rate from the laser. Furthermore, the beam quality is seen to deteriorate at higher repetition rates. The calculated temperature acceptance bandwidth is 2.5°C and the angular acceptance bandwidth $\Delta\varphi$ is 2°.

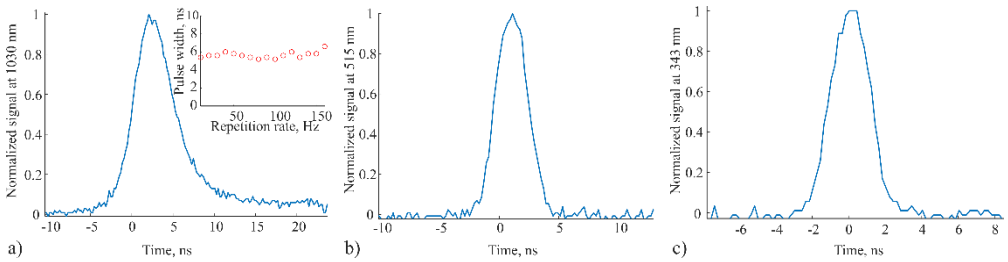

Fig. 4. a) Pulse profile of the 1030 nm with a FWHM of 5.4 ns; inset: pulse width of the 1030 nm as a function of repetition rate; b) pulse waveform of the 515 nm output with a FWHM of 3.2 ns; c) pulse waveform of the 343 nm output with a FWHM of 2.3 ns. All pulse profiles are measured at 100 Hz.

The pulse energy of the 343 nm laser increases from 2 µJ at 10 Hz to 26 µJ at 180 Hz repetition rate. The measured THG conversion efficiency (IR-UV) increases from 1 to 13% as shown in Fig. 3(c), red squares. We explain the reduced conversion efficiency measured at lower repetition rates as follows: the SHG crystal was not readjusted during the measurement of the SFG efficiency. Only the SFG crystal was slightly readjusted to compensate for the center wavelength fluctuations. Thus, the phase matching in the first crystal might be not optimal, particularly not at low repetition rates, as it was optimized for 180 Hz. The theoretically predicted IR-UV conversion efficiency is 22% at 100 Hz which is by a factor of 2 higher than measured. This is probably due to a misaligned overlap of the interacting

Optics EXPRESS

beams, or the uncertainty of the nonlinear coefficient. The calculated temperature acceptance bandwidth is 3.1°C and the angular acceptance bandwidth, Δθ is 0.08° for the SFG process. Figure 4 presents measured temporal profiles of the 1030 nm output, SHG and THG, with a FWHM of 5.4 ns, 3.2 ns and 2.3 ns, respectively. The UV beam after the collimating lens L4 is measured with the knife-edge method (data not shown). The beam is elliptic with radii of w_x = 1.54 mm and w_y = 0.95 mm, where w_x and w_y are radii defined at the intensity decrease of $1/e^2$. The effective area ($A_{eff} = \pi w_x w_y / 2$) is 2.3 mm^2 and the ellipticity is 1.5.

3.3. Time-resolved fluorescence immunoassays

The developed passively Q-switched laser at 343 nm is intended for time-resolved measurements of immunoassays. In such measurements, excitation and detection are separated in time to avoid fast background fluorescence and exploit the long lifetime of europium-based fluorophores (about 1 ms). In immunoassay diagnostics, measurements of very low analyte concentrations are of interest [19]. At these low signal levels, any noise sources and instabilities are relevant. Timing jitter and peak power fluctuation of the excitation light source contribute as noise sources to the fluorescence measurements. Therefore, in the following we investigate potential noise source contributions from the developed laser source.

The 1030 nm pulse-to-pulse peak power fluctuation is 1.6% calculated from >1000 measured optical pulses. The histogram and normal distribution curve are shown in Fig. 5(a). The Q-switched pulse is emitted approximately 1.9 ms after the positive edge of the pump pulse (operating at 100 Hz). The timing jitter of the 1030 nm pulses is 32.6 µs which is 0.3% relative to the cycle duration of 10 ms, used in europium-based systems. The 1030 nm timing jitter is measured as the standard deviation of the delay time distribution of >1000 optical pulses plotted in Fig. 5(b). Since the Q-switched pulse is emitted only about 100 µs before the end of the pump pulse, the pulse width fluctuation of the pump is also measured. The standard deviation of the pump pulse width is 2.5 µs. The fall time is 21.5 µs, calculated from an average of >1000 pulses, with a standard deviation of 114 ns. In addition, the diode pump pulse amplitude fluctuation is measured to be very low (0.06%). The timing jitter of a passively Q-switched system is fundamentally limited by the spontaneous emission noise [20]. Additional factors include pump pulse fluctuations, resonator mode fluctuations, and temperature fluctuations of the laser medium and consequently the emission wavelength [21–24]. A few methods of reducing timing jitter of passive Q-switched lasers have been suggested, such as the use of composite pump pulses [22] and bleaching the saturable absorber [23].

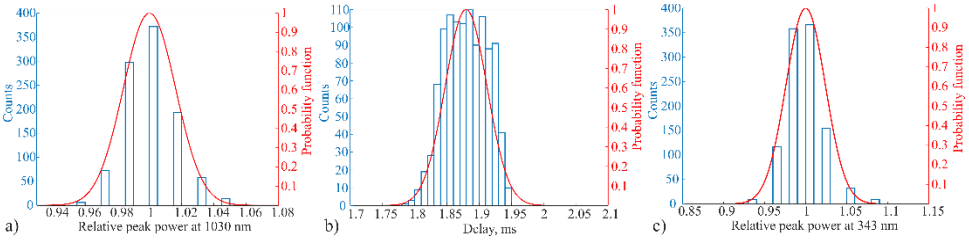

Fig. 5. a) Peak power distribution of 1030 nm pulses, >1000 measurements, pulse-to-pulse amplitude fluctuation is 1.6%; b) distribution of delay time of the Q-switched pulse relative to the positive edge of the pump pulse, >1000 measurements, average value 1.9 ms, standard deviation 32.6 µs, variation 1.7%; c) peak power distribution of the 343 nm laser output with a pulse-to-pulse amplitude fluctuation of 2.4% measured with >1000 pulses.

The distribution of the 343 nm pulse peak power values is measured using >1000 pulses, as shown in Fig. 5(c). The pulse-to-pulse peak power fluctuation is 2.4%. The accuracy of the peak power measurement is limited by the rise time of the detector. The peak power

Optics EXPRESS

fluctuation reflects the pulse-to-pulse energy fluctuation as the pulse width does not change at fixed repetition rate.

As mentioned before, the obtained cycle duration of 10 ms matches the decay lifetime of lanthanides which are often used in time-resolved fluorescence spectroscopy. The measured timing jitter is only 0.3% relative to the cycle of the measurement (10 ms) and 3.2% relative to a typical lifetime of europium (1 ms). We have calculated the impact of the timing jitter on the collected signal from a fluorophore with a decay lifetime of 1 ms. The timing jitter of 32 µs results in a fluctuation in the range of ± 3% of the emitted fluorescence signal, within one standard deviation and ± 7% within two standard deviations. Depending on the exact application this noise source can be neglected. For example, in our previous work we show that in a state-of-the-art time-resolved fluorescence immunoassay measurement system, the variation from sample to sample can be up to 6%, and from system to system up to 11% [19]. We note that the noise can be further reduced by signal averaging. For applications requiring higher sensitivity, or when employing short (nanosecond) lifetime fluorophores, the timing jitter noise factor can be avoided by optically triggering the detection circuit. With a peak power fluctuation of 2.4% the collected signal changes within 2.4% as well.

4. Conclusion

A low repetition rate, simple and cost-effective 343 nm solid-state laser source is developed through THG of a passively Q-switched diode-pumped Yb:YAG laser source. At 343 nm, pulse energy of 20 µJ, pulse width of 2.3 ns and operation at a repetition rate of 100 Hz is obtained, converted from 1030 nm with pulse energy of 190 µJ and pulse width of 5.4 ns. The conversion efficiency is 10.4% at 100 Hz which is comparable to that obtained with mode locked lasers. The UV laser emits pulses on demand and can be electronically synchronized with a detection circuit. The low repetition rate matches particularly the millisecond scale lifetime of lanthanide fluorophores, targeting applications in fluoroimmunoassays and time-resolved fluorescence spectroscopy. The 343 nm output targets the excitation peak of the lanthanides. To the authors' knowledge, this is the first demonstration of 343 nm passively Q-switched solid-state laser.

In addition, the obtained timing jitter can be neglected when using the long fluorescence lifetime (about 1 ms) fluorophores, i.e. lanthanides widely used in fluoroimmunoassays. The timing jitter, however, can be avoided by implementing an optical feedback system. The UV pulse-to-pulse peak power fluctuation is 2.4%. The impact of these noise sources can be further decreased by signal averaging. High spatial beam quality and narrow spectral emission of the laser will allow for further decrease of the unwanted background contributions in fluoroimmunoassay measurements.

For future work, the system will benefit from a frequency selective component stabilizing the output spectrum.

Funding

Innovation Fund Denmark (grant 4135-00118B).

References

1. J.-C. G. Bünzli, "Lanthanide luminescence for biomedical analyses and imaging," Chem. Rev. **110**(5), 2729–2755 (2010).
2. J. R. Lakowicz, *Principles of Fluorescence Spectroscopy* (Springer US, 2006).
3. O. Rodenko, H. Fodgaard, P. Tidemand-Lichtenberg, P. M. Petersen, and C. Pedersen, "340 nm pulsed UV LED system for europium-based time-resolved fluorescence detection of immunoassays," Opt. Express **24**(19), 22135–22143 (2016).
4. S. Sartania, Z. Cheng, M. Lenzner, G. Tempea, C. Spielmann, F. Krausz, and K. Ferencz, "Generation of 0.1-TW 5-fs optical pulses at a 1-kHz repetition rate," Opt. Lett. **22**(20), 1562–1564 (1997).
5. J. Rothhardt, C. Rothhardt, M. Müller, A. Klenke, M. Kienel, S. Demmler, T. Elsmann, M. Rothhardt, J. Limpert, and A. Tünnermann, "100 W average power femtosecond laser at 343 nm," Opt. Lett. **41**(8), 1885–1888 (2016).

Optics EXPRESS

6. J. P. Negel, A. Loescher, A. Voss, D. Bauer, D. Sutter, A. Killi, M. A. Ahmed, and T. Graf, "Ultrafast thin-disk multipass laser amplifier delivering 1.4 kW (4.7 mJ, 1030 nm) average power converted to 820 W at 515 nm and 234 W at 343 nm," Opt. Express **23**(16), 21064–21077 (2015).
7. J. Dong, K. Ueda, A. Shirakawa, H. Yagi, T. Yanagitani, and A. A. Kaminskii, "Composite Yb:YAG/Cr4+:YAG ceramics picosecond microchip lasers," Opt. Express **15**(22), 14516–14523 (2007).
8. J. Dong, Y. Ren, and H. Cheng, "> 1 MW peak power, an efficient Yb: YAG/Cr4+: YAG composite crystal passively Q-switched laser," Laser Phys. **24**(5), 055801 (2014).
9. M. Tsunekane and T. Taira, "High Peak Power, Passively Q-Switched Yb:YAG/Cr:YAG Micro-Lasers," IEEE J. Quantum Electron. **49**(5), 454–461 (2013).
10. B. Li, B. Sun, and H. Mu, "High-efficiency generation of 355 nm radiation by a diode-end-pumped passively Q-switched Nd:YAG/Nd:YVO_4 laser," Appl. Opt. **55**(10), 2474–2477 (2016).
11. D. N. Nikogosyan, *Nonlinear Optical Crystals: A Complete Survey* (Springer-Verlag, 2005).
12. M. Bass, L. S. Weichman, S. Vigil, and B. K. Brickeen, "The temperature dependence of Nd/sup 3+/doped solid-state lasers," IEEE J. Quantum Electron. **39**(6), 741–748 (2003).
13. O. Kimmelma, I. Tittonen, and S. C. Buchter, "Thermal tuning of laser pulse parameters in passively Q-switched Nd:YAG lasers," Appl. Opt. **47**(23), 4262–4266 (2008).
14. M. Tsunekane and T. Taira, "Temperature and polarization dependences of Cr:YAG transmission for passive Q-switching," Conference on Lasers and Electro-Optics and 2009 Conference on Quantum electronics and Laser Science Conference, Baltimore, MD, 2009, pp. 1–2.
15. K. Rottwitt and P. Tidemand-Lichtenberg, *Nonlinear Optics: Principles and Applications* (CRC Press, 2014).
16. K. Kato, "Tunable UV generation to 0.2325 mu m in LiB/sub 3/O/sub 5," IEEE J. Quantum Electron. **26**(7), 1173–1175 (1990).
17. S. P. Velsko, M. Webb, L. Davis, and C. Huang, "Phase-matched harmonic-generation in lithium triborate (LBO)," IEEE J. Quantum Electron. **27**(9), 2182–2192 (1991).
18. D. A. Roberts, "Simplified characterization of uniaxial and biaxial nonlinear optical crystals: a plea for standardization of nomenclature and conventions," IEEE J. Quantum Electron. **28**(10), 2057–2074 (1992).
19. O. Rodenko, S. Eriksson, P. Tidemand-Lichtenberg, C. P. Troldborg, H. Fodgaard, S. van Os, and C. Pedersen, "High-sensitivity detection of cardiac troponin I with UV LED excitation for use in point-of-care immunoassay," Biomed. Opt. Express **8**(8), 3749–3762 (2017).
20. S. L. Huang, T. Y. Tsui, C. H. Wang, and F. J. Kao, "Timing jitter reduction of a passively Q-switched laser," Jpn. J. Appl. Phys. **38**(3A), L239–L241 (1999).
21. D. Nodop, J. Limpert, R. Hohmuth, W. Richter, M. Guina, and A. Tünnermann, "High-pulse-energy passively Q-switched quasi-monolithic microchip lasers operating in the sub-100-ps pulse regime," Opt. Lett. **32**(15), 2115–2117 (2007).
22. J. B. Khurgin, F. Jin, G. Solyar, C. C. Wang, and S. Trivedi, "Cost-effective low timing jitter passively Q-switched diode-pumped solid-state laser with composite pumping pulses," Appl. Opt. **41**(6), 1095–1097 (2002).
23. B. Cole, L. Goldberg, C. W. Trussell, A. Hays, B. W. Schilling, and C. McIntosh, "Reduction of timing jitter in a Q-Switched Nd:YAG laser by direct bleaching of a Cr4+:YAG saturable absorber," Opt. Express **17**(3), 1766–1771 (2009).
24. M. W. Smillie, M. Silver, S. T. Lee, and T. J. Cook, "High single-pulse energy, passively Q-switched Nd:YAG laser for defence applications," Proc. SPIE **8959**, 89590Z (2014).